Thermal comfort modeling for smart buildings : a fine-grained deep learning approach

Zhang, Wei; Hu, Weizheng; Wen, Yonggang

2019

Zhang, W., Hu, W. & Wen, Y. (2019). Thermal comfort modeling for smart buildings : a fine-grained deep learning approach. IEEE Internet of Things Journal, 6(2), 2540-2549. https://dx.doi.org/10.1109/JIOT.2018.2871461

https://hdl.handle.net/10356/150840

https://doi.org/10.1109/JIOT.2018.2871461

Thermal Comfort Modeling for Smart Buildings: A Fine-Grained Deep Learning Approach

Wei Zhang, *Member, IEEE,* Weizheng Hu, and Yonggang Wen, *Senior Member, IEEE*

***Abstract*—The emerging internet of things (IoT) technology enables smart building management and operation to improve building energy efficiency and occupant thermal comfort. In this paper, we perform data analysis using the IoT generated building data to derive accurate thermal comfort model for smart building control. Deep neural network (DNN) is used to model the relationship between the controllable building operations and thermal comfort. As thermal comfort is determined by multiple comfort factors, a fine-grained architecture is proposed, where an exclusive model is trained for each factor and accordingly the corresponding thermal comfort can be evaluated. The experimental results show that the proposed fine-grained DNN outperforms its coarse-grained counterpart by 3.5× and is 1.7×, 2.5×, 2.4× and 1.9× more accurate compared to four popular machine learning algorithms. Besides, DNN's performance promotes with deeper network topology and more neurons, and a simple topology with the same number of neurons per network hidden layer is sufficient to achieve high modeling accuracy. Finally, the derived thermal comfort model reveals a linear relationship between comfort and air conditioning setpoint. The linear property helps quickly and accurately search for the optimal controllable setpoint with the desired comfort.**

***Index Terms*—Thermal comfort; smart building; smart city; deep learning.**

I. INTRODUCTION

BUILDING accounts for 40 percent of worldwide energy usage and 60 percent electricity usage [1]. A dominate fraction of the usage is contributed by the building's heating, ventilation and air conditioning (HVAC) system. In subtropical areas like Australia, HVAC even consumes about 70 percent of the building energy [2]. The chief purpose of the HVAC system is to maintain *thermal comfort* for the building occupants, who nowadays spend 90 percent of their time in buildings [3]. With poor comfort in buildings, occupants tend to suffer from sick building syndrome, absenteeism and cognitive degradation [4]. Thus, it is important to maintain a healthy and comfortable indoor environment for the well-being of the occupants and meanwhile minimize the building energy usage. A critical step towards this goal is to create accurate models for thermal comfort.

The most prevalent thermal comfort model should be the predict mean vote (PMV) proposed by Fanger et al. [5] and adopted in the ASHRAE Standard 55. PMV relates thermal comfort with six comfort factors, four indoor environmental ones including temperature, humidity, mean radiant temperature (MRT) and air velocity and two vital ones including metabolic rate and cloth insulation. Based on the factor values, the thermal comfort score can be calculated ranging from -3 to 3, where the seven integers in ascending order within the range indicate cold, cool, slightly cool, comfort, slightly warm, warm and hot.

Despite PMV's prevalence of thermal comfort modeling, it is not readily applicable to smart buildings. The comfort factors such as indoor temperature and humidity are not directly controllable variables of the HVAC system. Rather, they are the results of the complex synergy between the outdoor environment, HVAC controllable operations and the other parameters. For example, as we will show in the later part of this paper, the difference between the HVAC temperature setpoint and indoor temperature varies in time and can be significant in practice. Thereby in a typical smart building, the building management system (BMS) would like to emulate the resulting comfort level and energy consumption of a variety of controllable HVAC settings before the real deployment. Accordingly, the BMS can choose the best setting with satisfied comfort and minimized energy usage and deploys the corresponding controllable operations in real settings. Thus, new thermal comfort models which link comfort and the controllable HVAC operations need to be developed to realize the accurate smart building control.

Recent development of the internet of things (IoT) technology helps derive the new comfort models, where a wide spectrum of the IoT solutions already exsit in the market [6], [7], [8]. Many nowadays buildings are well instrumented with the IoT facilities to monitor the building conditions such as HVAC status, energy usage and ambient environment [9], [10], [11]. The building data is collected using the associated IoT data acquisition network and can be accessed by the BMS for online data analysis. In this paper, we aim to advance the thermal comfort modeling for smart buildings using the IoT generated building data and the deep neural network (DNN). As a popular deep learning algorithm, DNN has proved its excellent capability in the applications such as image processing, computer graphics and signal processing [12], [13]. This work tries to extend DNN's excellence to comfort modeling and investigates its feasibility for bridging the gap between the controllable HVAC operations and thermal comfort.

In addition, a fine-grained modeling architecture is proposed to promote the modeling accuracy. Most existing thermal comfort models adopt coarse-grained architecture, using only one model to link the input attributes and thermal comfort directly [14], [15]. In the proposed fine-grained architecture, an exclusive model is created and trained for each comfort factor

W. Zhang, W. Hu and Y. Wen are with the School of Computer Science and Engineering, Nanyang Technological University, 50 Nanyang Avenue, Singapore 639798. Email: wei.zhang@ieee.org and {huwe0012, ygwen}@ntu.edu.sg.

like temperature. Then the factor values from the multiple fine-grained models are combined to calculate the final thermal comfort score. To valid the soundness of our proposed fine-grained deep learning approach, extensive data analytics is performed using DNN and several other popular machine learning (ML) algorithms, including neural network (NN), linear regression (LR) and support vector machine (SVM) regression with linear kernel (SVR-L) and nonlinear RBF kernel (SVR-R). Key research findings are as follows:

- Fine-grained modeling outperforms the coarse-grained modeling for DNN by 3.5× and the other tested ML algorithms by over 20 percent.
- DNN's modeling accuracy promotes with more hidden layers and more neurons in the network topology, although a diminishing return of adding more layers and neurons is observed. Also, a simple topology with the same number of neurons per hidden layer is sufficient to produce remarkable performance compared to the more complex topologies.
- Thermal comfort model is not trivial in nature. Linear ML algorithms LR and SVR-L fail to deliver good modeling accuracy compared to the nonlinear algorithms DNN, NN and SVR-R. Besides, DNN achieves the best modeling accuracy with moderate time usage on model training. Compared to NN, LR, SVR-L and SVR-R, DNN is 1.7×, 2.5×, 2.4× and 1.9× more accurate, respectively. Also, thermal comfort is linearly related to the HVAC setpoint, which enables to compute the optimal setpoint for the desired comfort instantaneously.

While the main goal of this work is thermal comfort modeling and smart building control, the work also has other benefits like demand response and power grid stabilization. For example, during the peak hours with high energy demand and electricity price, the thermal comfort requirement can be relaxed to a certain extent with less energy usage, and vice verse. Corresponding accurate building control can be realized based on the derived thermal comfort model in this paper. This not only helps stabilize the power grid but also reduces the electricity bill of the building owners. Such benefits can be substantial as building serves as a dominant energy consumer of the grid.

The rest of this paper is organized as follows. We review related works in Section II. In Section III, we describe the adopted dataset and present the system architectures. Section IV investigates different modeling granularity and compares the performance of fine-grained modeling and coarse-grained modeling. Section V discusses the modeling performance using different network topologies for DNN. In Section VI, the modeling performance using different algorithms are studied. Based on the derived thermal comfort models, a case study of the smart building control is also presented in Section VI. Finally, Section VII concludes this paper and suggests several future research directions.

II. Related Works

Thermal comfort modeling has received much attention in the recent decades. The most widely adopted model should be PMV proposed by Fanger et al. [5] in the 1970s. ASHRAE Standard 55 [16] recommends the buildings to maintain a PMV within ± 0.5 for a comfortable environment.

While PMV score can be mathematically calculated with the six comfort factors, recent studies also try to use ML to model the relationship between the factors and score. Megri et al. in [14] achieve the goal using ε-SVM. Tested on a small-scale dataset with less than 800 training samples and less than 20 testing samples, the proposed ε-SVM comfort modeling can approximate the PMV calculations by up to 99%. Similarly, Atthajariyakul and Leephakpreeda in [15] investigate the feasibility of using NN. A network topology with two hidden layers are adopted and the derived model also approximates the PMV model well. Besides, other comfort factors such as gender and age are incorporated to improve the modeling accuracy [17], [18]. Hu et al. in [19] monitor the occupant vital signals like heartbeat rate using wearable devices and predict thermal comfort accordingly using NN.

PMV model is also inverted to derive the comfortable temperature, which is often assumed to be equal to the HVAC setpoint. In [20], Javed et al. adopt the random neural network (RNN), where the indoor temperature is the target to model and the PMV score as well as the rest five comfort factors are used as the input attributes. Besides, some works avoid the complex PMV calculations by assuming certain simplified thermal comfort models, i.e., a quadratic function of the difference between the indoor temperature and the most comfortable temperature [21].

Despite the progress of thermal comfort modeling, the above works are parameterized by the comfort factors unable to be controlled directly. To realize smart building control, this paper aims to model the relationship between the controllable HVAC operations and thermal comfort. So that the BMS can use the derived model to emulate the thermal condition with different operational settings, and accordingly choose the best one for real deployment.

III. Data Description and System Architectures

In this part, a building dataset adopted in this paper is introduced first. Then, the system architectures of thermal comfort modeling are presented.

A. Dataset

This work adopts a publicly available dataset from an IoT instrumented building [22], and the results shown in this paper can be reproduced using the dataset. The dataset is collected at an office building in Center City Philadelphia, USA and spans for one year from July 2013 to July 2014. In total there are 678,621 data samples in the dataset, and the attributes associated with the data samples are grouped into the following categories.

1) Datetime Attributes: The raw dataset includes a string-based datetime attribute. To facilitate the data processing in ML algorithms, datetime is digitalized into three attributes, including the integer-based year, month and weekday.

2) Outdoor Attributes: Three outdoor attributes available in the dataset are the temperature in Celsius, relative humidity as a percentage and air velocity in m/s.

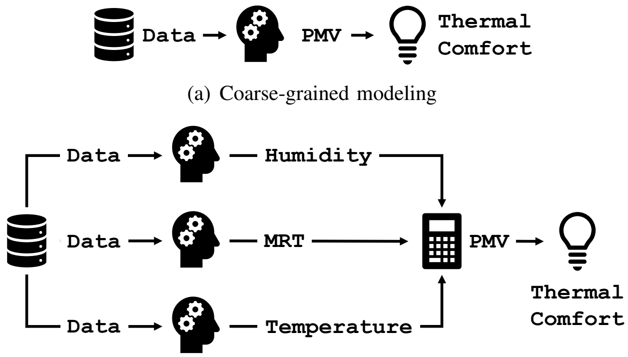

(a) Coarse-grained modeling

(b) Fine-grained modeling

Fig. 1. System architectures of the coarse-grained and fine-grained thermal comfort modeling.

3) HVAC Attributes: There are two HVAC attributes, cooling setpoint and heating setpoint, both in Celsius. Cooling and heating setpoints represent the configured ideal indoor temperature under HVACs cooling mode and heating mode, respectively, and normally the former is higher than the later.

4) Indoor Attributes: The dataset also has three attributes to evaluate the indoor environment, including temperature and MRT in Celsius and relative humidity in percentage.

In this paper, we define a typical valid range for each attribute, i.e., weekday between 1 and 7 with 1 indicating Monday, indoor temperature between 10 and 35 Celsius degree, relative humidity between 10% and 90% and outdoor temperature between -15 and 40 Celsius degree. The data samples with any attribute value beyond the pre-defined range are treated as outliers and filtered out. We use the datetime, outdoor and HVAC attributes as the input attributes for training the thermal comfort models. The indoor attributes are taken as the ground-truth of the target attributes for model training. Details will be presented in the following part.

B. System Architectures

In this part, two thermal comfort modeling architectures are introduced and illustrated in Fig. 1. The coarse-grained one is shown in Fig. 1(a), where the data system feeds the attributes for datetime, outdoor and HVAC to the ML algorithm as the inputs and the PMV-based comfort scores as the target.

Here, the PMV score can be computed based on the three indoor attributes. Since an office building is considered in the dataset, this paper follows the general assumption that indoor air velocity, occupant metabolic rate and cloth insulation are unchanged during a long enough period and can be deemed as given. Specifically, air velocity and metabolic rate are assumed to be 0.1 m/s and 1.2, respectively, in a typical office setting.

The architecture in Fig. 1(a) aims to model a direct relationship between the input attributes and thermal comfort. Differently, the second architecture in Fig. 1(b) explores the relationship at finer granularity. An exclusive ML model is introduced to model the relationship between the input attributes and each of the thermal comfort factors, including indoor temperature, indoor humidity and indoor MRT. Here, the historical data of the three indoor attributes are used as the ground-truth of the target values. Then, the modeled factor values can be inputted into the PMV calculator to derive the corresponding comfort score. The details of the PMV calculations can be found in [5].

The derived thermal comfort model helps realize the smart building control. Given any datetime and ambient condition, we can use the model to test the resulting thermal comfort scores of different building configurations, i.e., HVAC settings. Then, the configuration with satisfied comfort and high energy efficiency can be selected to deploy in real setting.

The following part will compare and discuss the performance difference of the coarse-grained modeling and the fine-grained modeling.

IV. THERMAL COMFORT MODELING GRANULARITY

In this section, the two system architectures are investigated for their comfort modeling performances using DNN.

A. Experimental Settings

The algorithm and experiment in this paper are implemented in Python 3.6. The data samples are divided into the training dataset with 75 percent samples and the testing dataset with 25 percent samples. The input attributes for both architectures are normalized. DNN is configured with one input layer with 8 neurons to match with the 8 input attributes, 10 hidden layers each with 300 neurons and one output layer with one neuron for the modeling target. 10 percent of the training data is used as the validation data in each DNN iteration. Experiments are conducted on a laptop running 64-bit Windows 10 Pro on an Intel Core i5-7300U CPU and using 16 GB of memory.

The performance is evaluated using two metrics, mean absolute error (MAE) and *improvement*. The later is defined as follows. Given two solutions A and A', achieving the modeling error of ε and ε', respectively, A's improvement to A' is ε'/ε. An improvement larger than 1 means A performs better than A' with smaller modeling error, and vice verse.

B. Algorithms with Different Modeling Granularity

Although the same DNN algorithm is used, the comfort modeling performance varies with different modeling granularity. Here, the following eight algorithm settings are adopted to investigate the impact of modeling granularity.

The first setting denoted as DALL is based on the fine-grained architecture as shown in Fig. 1(b), where three comfort factors are modeled. Then, DALL is modified to model two of the three factors and three settings DTH, DTM and DHM can be derived, where the subscripts T, H and M represent indoor temperature, humidity and MRT, respectively. For example, DTH implies that temperature and humidity are modeled and such implication applies to DTM and DHM also. If not modeled using DNN, temperature and MRT are assumed to be equivalent to the middle value of the HVAC's cooling setpoint and heating setpoint, and humidity is assumed to be a moderate value of 50%. Similarly, three more variants DT, DH and DM are introduced, which models only temperature, humidity and MRT, respectively. Lastly, the coarse-grained architecture in Fig. 1(a) is considered to model the PMV-based comfort score directly, denoted as DPMV.

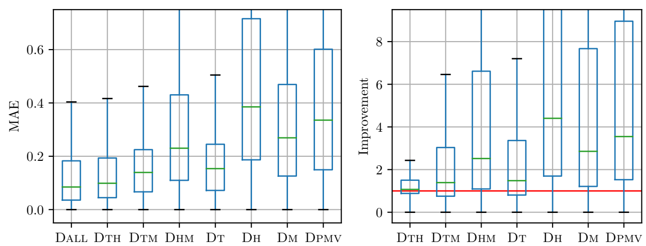

(a) (b)

Fig. 2. The modeling error of DNN with different modeling granularity in Fig. 2(a) and DALL's improvement to the other settings in Fig. 2(b). The improvement of 1 is indicated by a red horizontal line in Fig. 2(b).

C. Results with Different Modeling Granularity

The results of the above-introduced algorithm settings are shown in Fig. 2. Fig. 2(a) shows the algorithms' MAE of 10 independent runs. Fig. 2(b) selects a random run and reports DALL's improvement to the remaining settings for every test data sample in the random run.

In Fig. 2, DALL achieves the best modeling accuracy with an average MAE of merely 0.13 and a median MAE of 0.08. For the PMV variance within such tiny range, even occupants may not be able to tell the difference subjectively.

Removing any comfort factor from modeling, the accuracy suffers. For DTH, DTM and DHM, the median[1] MAEs are 0.10, 0.14 and 0.23, respectively, larger than DALL's 0.08. Among the factors, the temperature has the highest impact on the overall modeling accuracy. DALL is 2.5× better than DHM without modeling temperature. When MRT and humidity are not modeled, DALL is only 7.1 and 39.0 percent better than DTH and DTM, respectively. This is reasonable, as the temperature has a more direct impact on the thermal environment compared to humidity and MRT.

The modeling performance further degrades when two factors are not modeled, where DT, DH and DM are generally noncompetitive to DALL and DTH, DTM and DHM without only one factor to model. The median MAEs for DT, DH and DM are 0.15, 0.39 and 0.27, respectively, and DALL outperforms them by 1.5×, 4.4× and 2.9× regarding the median improvement.

Lastly, the coarse-grained modeling DPMV fails to model thermal comfort accurately and the performance gap to the fine-grained DALL is significant. Seen from Fig. 2, DPMV achieves a median MAE of 0.34 which is better than only DH, where only humidity is modeled. DPMV's fine-grained counterpart DALL achieves a median improvement of 3.5×.

Overall, fine-grained modeling at comfort factor level is the right choice for advancing the comfort modeling accuracy. In this scenario, the thermal comfort model can be decomposed into several building blocks, such as temperature model and humidity model, which are relatively easier to be modeled with higher accuracy. It is also important to explore more between the input attributes and comfort factors, as modeling more factors reveals more performance advantage than modeling fewer.

[1]Median values are selected for results analysis and discussion in some parts of this paper, as the mean values could be drifted substantially by the results outliers, which however only occur rarely.

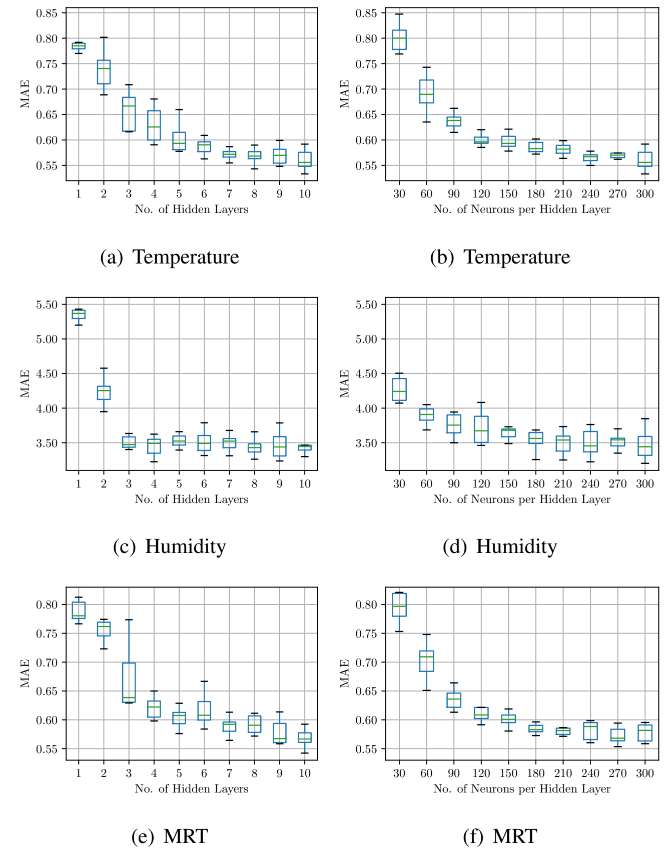

(a) Temperature (b) Temperature

(c) Humidity (d) Humidity

(e) MRT (f) MRT

Fig. 3. DNN's modeling performance with different network topologies. Figs. 3(a), 3(c) and 3(e) show the factor modeling results with 300 neurons per hidden layer and the number of layers varies between 1 and 10. Figs. 3(b), 3(d) and 3(f) show the results with 10 hidden layers and the number of neurons per hidden layer varies between 30 and 300.

V. DNN TOPOLOGY

In this section, DNN topology is investigated in detail to find out the ones with remarkable modeling performance.

A. Network Depth and Width

Two critical DNN topology parameters are the network depth and width or the number of hidden layers and the number of neurons per hidden layer. Generally, small network due to its limited capacity cannot contain sufficient information to approximate the real system model. This is especially true when the modeled system is complex. However, large network sometimes also fails to derive good performance due to the reasons like over-fitting, where the trained model is biased by the training data and becomes unfit for the testing data. In this part, different DNN topologies are tested with the network depth varies between 1 and 10 and the width varies between 30 and 300. The results are shown in Fig. 3.

1) Network Depth: The performance impact of the network depth is shown in Figs. 3(a), 3(c) and 3(e). Seen from the figures, DNN's modeling performance improves with more hidden layers. The median MAE for indoor temperature improves from 0.78 °C with one hidden layer to 0.56 °C with ten hidden layers, with around 40 percent improvement. Similar values also apply to MRT. For humidity, it improves from 5.4% to 3.4%, around 60 percent improvement. The reason could be that more layers allow the modeled system to be decomposed into more information building blocks easier to be interpreted.

However, the improvement slows down with more layers added. For temperature and MRT, the MAE improvement becomes insignificant with more than five hidden layers. While the median MAE for temperature modeling shows a 32 percent decrease from 0.78 °C with one hidden layer to 0.56 °C with five layers, doubling the number of hidden layers to ten only achieves a 5.4 percent decrease with 0.03 °C modeling accuracy variation. For humidity, such phenomenon occurs even earlier since three hidden layers. After over 50% improvement from one hidden layer to three, the median MAE of humidity modeling merely varies from 3.5% to 3.4% with seven more hidden layers added. Such diminishing return also implies that the temperature and MRT models are more complex compared to humidity and the models' return from more layers diminishes much slower.

Besides, none of the factor models suffers from over-fitting and the modeling performance does not degrade with more hidden layers. One reason should be that our dataset is large enough. With over half million data samples, it is less likely that certain characteristics are only contained in the training data instead of existing in both training data and testing data. So, the derived models are not biased by the training data and keep improving with more neurons.

2) Network Width: Following the discussion on network depth, this part studies the performance impact of network width, or the number of neurons per hidden layer. Figs. 3(b), 3(d) and 3(f) show the results with ten hidden layers and the width varies between 30 and 300. Same as the finding for network depth, the modeling performance benefits from more neurons as the network widens. Also, the improvement saturates with more neurons added.

One interesting fact is that the convergence speed in network width seems faster than that of the network depth. Take temperature for example. Doubling one hidden layer to two layers decreases the median MAE from 0.78 °C to 0.74 °C by 5.4 percent, and further doubling to four layers improves the MAE to 0.63 °C by 17 percent. Regarding the network width, the first doubling, from 30 neurons to 60 neurons, reduces the MAE to 0.69 °C by 16 percent and further doubling to 120 neurons achieves a 0.60 °C median MAE with 15 percent improvement. Similar behavior can also be observed for MRT. One reason is that the increase in the number of hidden layers and the number of neurons per hidden layer have the different impact on Dnn. In Dnn, the neurons between two adjacent layers are fully connected, producing $O(mn^2)$ neuron links in total for m hidden layers and n neurons per layer. Dnn's modeling capability normally scales in the number of neuron links, which are the basic units to record model information. Such link amount scales linearly in the network depth, but exponentially in the network width. As a result, the performance change is more significant as the network widens and relatively less significant as the network deepens.

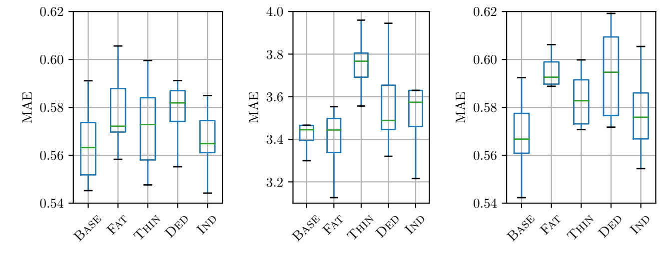

(a) Temperature (b) Humidity (c) MRT

Fig. 4. The factor modeling performance using Dnn with the same amount of 3,000 neurons and different network topologies.

B. Neuron Allocation

More neurons promote the comfort modeling performance as shown above. In this part, let us discuss the optimal allocation of the neurons to each hidden layer.

1) Topology Description: Five topologies with different neuron allocations are investigated given the same total number of neurons, i.e., 3,000. The first one, denoted as Base, evenly distributes the neurons to ten hidden layers, so each layer has 300 neurons. The second one denoted as Fat squeezes the topology into less hidden layers but each layer has more neurons; specifically, five hidden layers each with 600 neurons. The third one denoted as Thin stretches the topology of Base into 20 hidden layers each with 150 neurons. The rest two topologies do not assume the evenly distributed neurons. One is Ded, which assumes a deductive topology where the information decomposes into finer units for deeper hidden layers. The number of neurons of Ded increases as 100, 100, 200, 200, 300, 300, 400, 400, 500 and 500 from the first hidden layer adjacent to the input layer to the tenth hidden layer. The other one Ind assumes an inductive information diffusion with the number of neurons in an reverse order as Ded for the ten hidden layers.

2) Performance Comparison: The modeling performance for the three comfort factors using different topologies introduced above is shown in Fig. 4. For the temperature modeling results shown in Fig. 4(a), Base achieves the best overall performance with a median MAE of 5.6 °C, which is 1.6, 1.7, 3.3 and 0.9 percent more accurate than Fat, Thin, Ded and Ind, respectively. Similar observation can also be found for the humidity and MRT modeling.

One implication is that Base evenly distributes the same number of neurons to each of the ten hidden layers is sufficient, or even the best, for Dnn to achieve a superior modeling performance. While Ded and Ind make certain assumptions such as deductive and inductive information diffusion, it turns out that the assumptions are not true enough and the diffusion process can be more complex. As a result, a general topology as in Base, although simple and unadorned, can well cover and model the complexity in the modeled systems of different comfort factors.

Besides, a fatter or thinner general topology like Base does not help improve the modeling performance. Such observation

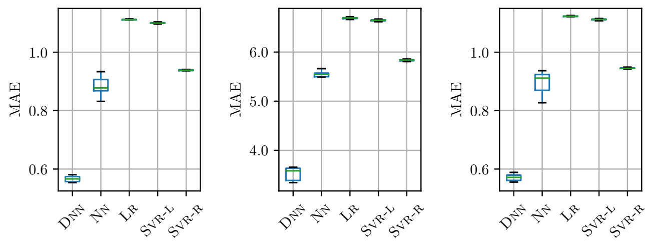

(a) Temperature (b) Humidity (c) MRT

Fig. 5. Comfort factor modeling performance using different ML algorithms.

TABLE I
THE TIME CONSUMPTION IN HOURS OF MODEL TRAINING FOR THE COMFORT FACTORS USING DIFFERENT ALGORITHMS. MEAN VALUES AND STANDARD DEVIATIONS (STD) ARE REPORTED.

	Temperature	Humidity	MRT
Algorithm	Mean (STD)	Mean (STD)	Mean (STD)
DNN	1.26 (0.27)	0.97 (0.16)	1.31 (0.22)
NN	0.19 (0.11)	0.28 (0.05)	0.16 (0.11)
LR	<0.01 (<0.01)	<0.01 (<0.01)	<0.01 (<0.01)
SVR-L	5.85 (0.75)	3.27 (0.08)	6.21 (0.72)
SVR-R	15.97 (3.64)	15.60 (2.50)	9.17 (4.06)

suggests that the number of hidden layers and the number of neurons per layer should be configured to moderate values. In practice, trial tests can be conducted to find out a good value pair, i.e., 10 hidden layers each with 300 neurons.

Specifically for humidity modeling in Fig. 4(b), THIN performs much worse than its counterparts BASE and FAT with less layers. This observation complies with the finding in Fig. 3(c), where the humidity modeling error converges fast and quickly stops improving since three hidden layers. Thus, the DNN topology can be application-dependent and the best topology may differ for different applications.

Overall, the simple topology like BASE by allocating the same number of neurons to each hidden layer is adequate for DNN to achieve the performance excellence. In addition, DNN performs quite stable with different tested topologies, with less than 5 percent difference for the majority of the tests. Stability is often a critical consideration in real applications and implementations, and DNN for the sake of this can be a suitable algorithm also.

VI. MODELING PERFORMANCE

Based on the above-derived conclusions, this section adopts the fine-grained modeling architecture and DNN with a general topology with the same number of neurons per hidden layer. The corresponding performance is investigated in detail.

A. *Comfort Factor Modeling Performance*

Four well-known ML algorithms are introduced for performance comparison, including two linear ones LR and SVR-L and two nonlinear ones SVR-R. Let us describe the algorithm settings first.

1) Algorithm Configuration: DNN is configured with 10 hidden layers each with the same 300 neurons according to the conclusions in Section V. The four ML algorithms are implemented using `scikit-learn` with the default settings, i.e., NN is configured with one hidden layer and a hundred neurons in the layer. Although the default settings may not necessarily achieve the best performance, they are empirically effective for the majority of the general applications. This work thus adopts the default settings for generality.

2) Modeling Accuracy Comparison: Fig. 5 shows the factor modeling performance for different comparison algorithms.

DNN achieves the best performance for modeling all the three comfort factors, compared to the four comparison algorithms. DNN's median MAE is merely 0.56 °C for indoor temperature and such performance is 55, 96, 94 and 66 percent better than NN, LR, SVR-L and SVR-R, respectively. Similar improvements also apply to the MRT modeling. For humidity, DNN is 55, 87, 86 and 63 percent better than the four comparison algorithms, respectively. The results show that DNN can well exploit the relationship between the input attributes and target comfort factors with a deeper and wider network. The comparison algorithms, although popular and have been widely deployed in practice, seem to fail to discover the subtle details well as DNN does and makes much higher modeling error compared to DNN.

NN with a shallow network performs the best among the four comparison algorithms. This shows that neural network related algorithms such as DNN and NN are quite suitable for comfort factor modeling. The shallow one offers a relatively sound basis for DNN to further improve the modeling performance. Nevertheless, the results also reveal the insufficiency of using a shallow network, i.e., one hidden layer only, for factor modeling and more complex networks are necessary for achieving higher modeling accuracy.

Besides, the relationship between the input attributes and target comfort factors should not be trivially linear. According to the results, LR and SVR-L assuming a linear relationship perform poorly compared to the rest three algorithms, which assume a nonlinear relationship. Even compared to the worst performed nonlinear algorithm SVR-R, the two linear ones have almost 20 percent higher error for the temperature and MRT modeling, and almost 15 percent higher for humidity.

3) Time Consumption Comparison: Besides modeling accuracy, modeling time consumption is also a critical consideration for applying a solution in practice. Thus, this part presents the time consumption results for the tested algorithms for modeling training. The time of testing is not discussed here since testing normally finishes instantaneously. Table I shows the results.

Seen from the table, with over half million data samples for training, DNN still maintains a manageable time consumption of around one hour for one comfort factor. In practice, the models are often updated infrequently, i.e., several hours or even days. While the time results here are obtained with a common laptop, the training process can also be accelerated with the high-end computing machines and high-performance computing technologies. Regarding the time complexity, DNN is linear in the number of data samples given a fixed number of optimization iterations. Thus, DNN can sustain for the even larger dataset in the future.

Humidity modeling by DNN takes less than one hour and is faster compared to the temperature and MRT modeling, each taking 30 and 35 percent more time, respectively. One reason could be that the humidity model is relatively not complex and can be well modeled even with only three hidden layers as indicated in Fig. 3(c).

NN and LR run much faster than DNN. Especially for the later one, which takes only a couple of seconds to finish. Nevertheless, it sounds to achieve better modeling performance for evaluating occupant comfort level more accurately, as long as the time consumption is manageable.

The two SVR variants are significantly slower compared to the other comparison algorithms. For SVR-L with the linear kernel, over 3 hours are used for humidity modeling and around 6 hours for temperature or MRT. With a nonlinear kernel, SVR-R is even slower, consuming around 10 hours for modeling MRT and over 15 hours for temperature or humidity. SVR's slowness is due to its quadratic time complexity in the number of data samples so that SVR is unsuitable for large datasets like the one used in this work. With more data available in the future applications, SVR can be even slower and as a result becomes impractical to be adopted.

B. Attribute Importance for Comfort Factors

Fine-grained modeling at comfort factor level is adopted in this work. Let us first investigate the importance of each input attribute to the target factor. Fig. 6 shows the F-score of each input attribute to the modeled factor using univariate analysis.

1) Indoor Temperature and MRT: Indoor temperature and MRT share the same attribute ranking and let us discuss the results of the two factors first.

a) Outdoor Attributes: It is interesting to find out that the outdoor temperature has the highest impact. Many existing works assume the equivalence among the HVAC setpoint, indoor temperature and MRT [23], [24]. However, the results in Fig. 6 show that the other attributes like outdoor temperature can have an even stronger impact on the indoor temperature and MRT. This motivates us to consider the weather condition in DNN for better modeling the comfort factors.

Another outdoor attribute, outdoor air velocity, also has a significant impact. While the air dynamics outside intuitively is not well related to the indoor thermal status, it is correlated with the outdoor temperature, which as shown above impacts the factor modeling a lot. Indeed, air movement is essentially due to the geographical temperature difference [25]. Despite the remarkable correlation between outdoor temperature and air velocity, the third outdoor attribute, outdoor humidity, is hardly correlated with the indoor temperature and MRT.

b) HVAC Attributes: Two HVAC attributes are among the top ranked attributes. This is reasonable because that the indoor air is directly conditioned by the HVAC system using the setpoints. Heating setpoint ranks higher than the cooling counterpart, and the reason could be as follows. The data used in this work is collected in Philadelphia, a subtropical city, where the cold periods is longer than the hot periods. Consequently, heating plays a more critical role than cooling for air conditioning. Such ranking can vary with different geographical areas. Note that either heating setpoint for warming air or cooling setpoint for cooling down air is effective at a time depending on the indoor thermal condition. Considering the full-time scale, the two HVAC setpoints together could be higher correlated with the indoor thermal environment than the individual correlation.

c) Datetime Attributes: Three datetime attributes are considered. The top correlated one is month, while the rest two, weekday and year, are less correlated. Such correlation could be due to the fact that outdoor temperature is strongly correlated with month, i.e., a high temperature in July and low in December. Outdoor thermal environment and indoor HVAC regulation together determine the indoor thermal condition.

2) Indoor Humidity: While the indoor temperature and MRT share the same attribute ranking, humidity shows a totally different ranking except for the outdoor temperature.

Outdoor attributes rank higher for modeling humidity than temperature and MRT. Outdoor humidity, as the least correlated attribute for temperature and MRT, ranks much higher for indoor humidity modeling. Many existing HVAC systems do not operate for adjusting humidity. Indoor humidity change often is a consequence of air ventilation, where a portion of the conditioned air is inhaled from the outside environment to maintain the fresh indoor air. As a result, the outdoor humidity has a substantial impact on the indoor humidity. Due to the similar reason, HVAC attributes, to the contrary, rank lower for humidity modeling. This again reveals the fact of HVAC's low regulation on indoor humidity in the tested case.

Datetime attributes play an important part for humidity modeling also, where the month and year attributes show stronger impact than the weekday attribute. Typically, humidity does not vary too frequently like temperature does in day and night. The variation of humidity often occurs monthly or seasonally, i.e., dryer air in winter and moist atmosphere in summer. This helps to explain the observation that the long-scale month and year attributes achieve high rankings.

C. Thermal Comfort Modeling Performance

Based on the derived models for comfort factors, the PMV-based thermal comfort score can be computed and the performance of different comparison algorithms is discussed here. Experimental results regarding the MAE of ten independent runs and DNN's improvement on every testing data samples of a random run are shown in Fig. 7.

DNN as well as the four comparison algorithms, including NN, LR, SVR-L and SVR-R, are investigated here, assuming a fine-grained architecture. Also, a variant assuming coarse-grained architecture is implemented for each of the four comparison algorithms, and let the variant names be CNN, CLR, CSVR-L and CSVR-R. Seen from Fig. 7, we have the following observations.

First, Fig. 7 reaffirms that fine-grained architecture at comfort factor level outperforms its coarse-grained counterpart. Regarding the mean MAE, the fine-grained NN, LR, SVR-L and SVR-R are 21, 20, 21 and 23 percent better than the coarse-grained CNN, CLR, CSVR-L and CSVR-R, respectively.

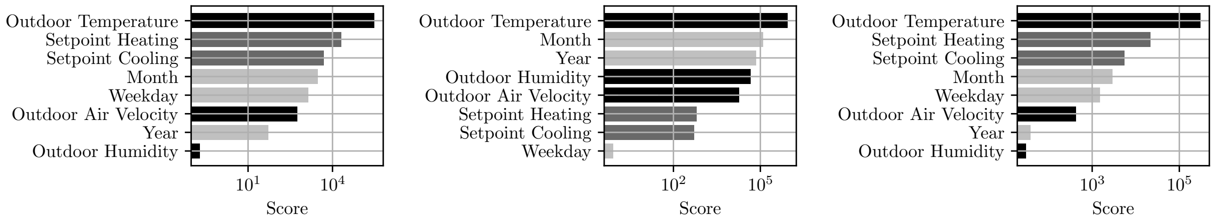

(a) Temperature (b) Humidity (c) MRT

Fig. 6. The F-score of each input attribute to the modeled comfort factor in descending order. High score means strong correlation.

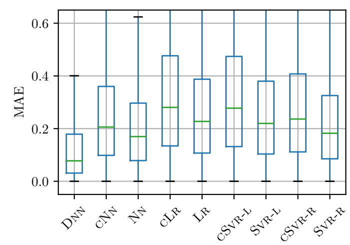

(a) (b)

Fig. 7. The thermal comfort modeling performance of DNN with fine-grained architecture and the comparison algorithms. NN, LR, SVR-L and SVR-R adopt the fine-grained architecture and cNN, cLR, cSVR-L and cSVR-R use the coarse-grained architecture. The improvement of 1 is indicated by a red horizontal line in Fig. 7(b).

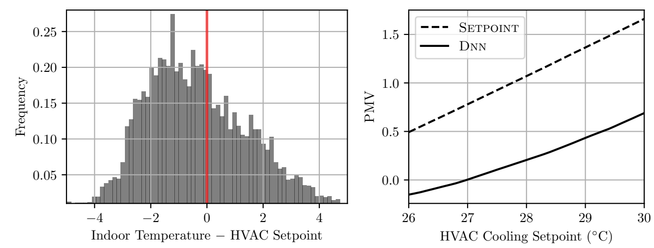

(a) (b)

Fig. 8. Fig. 8(a) shows the distribution of the temperature difference between indoor temperature and HVAC setpoint. Negative (positive) value means indoor temperature is lower (higher) than the HVAC setpoint. The difference of 0, or the equivalence between the indoor temperature and HVAC setpoint, is indicated by a red vertical line in Fig 8(a). Fig. 8(b) demonstrates the smart HVAC control where comfort changes with HVAC setpoint.

Such fact has been observed in Section IV using DNN and Fig. 7 shows that it also applies to other ML algorithms. This again indicates that fine-grained architecture is good at exploring the detail information within the modeled system, and such information helps model the relationship between the input attributes and thermal comfort more accurately.

With the same fine-grained architecture, DNN performs the best among the tested algorithms for thermal comfort modeling. The observation shows that DNN's superior performance on factor modeling as shown in Section VI-A is well inherited by the subsequent thermal comfort calculation. The mean MAE for DNN is merely 0.1 for the PMV score ranging between -3 and 3 and the other algorithms' mean errors are over twice higher. Regarding the median improvement, DNN is 1.7×, 2.5×, 2.4× and 1.9× better than NN, LR, SVR-L and SVR-R, respectively. Also, DNN not only performs better in general, it also achieves better performance for most of the testing data samples compared to the other algorithms. As shown in Fig. 7(b), DNN's improvement seldom goes below 1 and DNN is rarely inferior to the comparison algorithms.

Besides, nonlinear algorithms, DNN, NN and SVR-L, perform better than the linear ones, LR and SVR-R. This complies with the finding in Section VI-A also. Thus, as an application with a complex system, thermal comfort modeling should better be conducted using nonlinear ML algorithms and the trivial linear ones are not suitable enough.

D. Smart HVAC Control Demonstration

In this part, we investigate the divergence between the indoor temperature and HVAC setpoint. Then, we demonstrate the smart building control using the DNN-based thermal comfort model and how DNN deals with the divergence in reality.

First, the indoor temperature has a significant difference to the HVAC setpoint. Fig. 8(a) shows the difference distribution when the outdoor temperature is above HVAC's cooling setpoint. As we can see, indoor temperature can even be 5 °C lower or higher than the setpoint. Also, the air is often overcooled by the HVAC system, where indoor temperature is more likely to be much lower than the cooling setpoint. While indoor temperature is often assumed to be equivalent to the setpoint [23], [24], Fig. 8(a) shows that the assumption can be far from true in reality. To alleviate or even avoid such divergence, this work adopts DNN to model the comfort factors like indoor temperature, instead of making some unrealistic assumptions.

Fig. 8(b) shows the comfort score change in HVAC cooling setpoint for a summer workday morning, with 30 °C outdoor temperature, 60% humidity and 5.0 m/s air velocity. Two schemes are tested. The first one is SETPOINT, which follows the commonly adopted assumption that the setpoint, indoor temperature and MRT are equivalent. The second one is DNN, which models the complex system among the controllable HVAC setpoints, outdoor and the indoor condition. Seen from the figure, SETPOINT has a biased estimation of the indoor environment and tends to assume a warmer situation compared to DNN. The key reason is that SETPOINT does not capture the divergence between the actual indoor temperature and the HVAC setpoint, despite the fact that the air is often over-cooled in the tested case. Different from SETPOINT, DNN learns the complex thermal dynamics and derives more accurate thermal comfort model. Then, DNN tends to choose a relatively higher setpoint than SETPOINT to avoid over-cooling and maintain a comfortable indoor environment.

Typically, there exists a trade-off between energy and comfort, where better comfort means more energy usage. Assuming a cooling mode, the energy consumption is normally a decreasing function in HVAC setpoint, but discomfort is increasing. Here, the maximum acceptable comfort level can be specified, i.e., PMV score of 1.0 indicating a slightly warm indoor environment, to minimize the conditioning energy consumption as much as possible. Accordingly, the corresponding setpoint with the minimized energy usage and satisfied thermal comfort can be derived using the comfort model. Besides, suppose an energy model accurate enough is given, it is also possible to figure out the setpoint given certain energy quota for air conditioning.

In addition, an approximately linear relationship between the PMV-based comfort score and setpoint can be observed in Fig. 8(b). Accordingly, given a desired comfort score, the optimal setpoint can be computed from testing any two different setpoints. For example, the setpoint x can be set to 29.2 °C for the PMV of up to 0.5, where the PMV is 0.43 for setpoint 29.0 °C and 0.69 for 30.0 °C and $(0.5 - 0.43)/(x - 29.0) = (0.69 - 0.5)/(30.0 - x)$. Our un-optimized Python code can finish such computation instantaneously.

VII. CONCLUSION

In this paper, we revisit thermal comfort modeling using deep learning for the IoT instrumented buildings. Fine-grained modeling is proposed to train an exclusive model for each comfort factor and accordingly the thermal comfort score can be derived. We show that fine-grained modeling outperforms the coarse-grained counterpart significantly, which only produces one model to link the input attributes and the thermal comfort directly. Such fact not only applies to DNN but also the other ML algorithms. The impact of DNN topology is investigated. The results show that the modeling performance benefits from more hidden layers and more neurons. Also, a simple topology with the same number of neurons per hidden layer is sufficient to achieve higher modeling accuracy, compared to the more complex topologies. Thermal comfort model is shown to be complex and nonlinear. Linear ML algorithms such as LR and SVR-L fail to produce stronger performance compared to the nonlinear ones such as DNN, NN and SVR-R. Among the tested algorithms, DNN achieves the highest accuracy with reasonable time usage. Overall, DNN is 1.7×, 2.5×, 2.4× and 1.9× better than NN, LR, SVR-L and SVR-R, respectively, for thermal comfort modeling. In addition, thermal comfort score scales linearly in the HVAC setpoint, and this allows to search for the optimal setpoint quickly and accurately with the desired comfort.

In the future, we plan to study the impact of the other factors like occupancy to thermal comfort. We also would like to incorporate the latest technologies like wearable devices for thermal comfort modeling. Finally, we want to extend this work to building energy modeling.

REFERENCES

[1] W. H. Sadid, S. A. Abobakr, and G. Zhu, "Discrete-event systems-based power admission control of thermal appliances in smart buildings," *IEEE Transactions on Smart Grid*, vol. 8, no. 6, pp. 2665–2674, 2017.

[2] A. Ahmad, M. Hassan, M. Abdullah, H. Rahman, F. Hussin, H. Abdullah, and R. Saidur, "A review on applications of ann and svm for building electrical energy consumption forecasting," *Renewable and Sustainable Energy Reviews*, vol. 33, pp. 102–109, 2014.

[3] Z. Wu, Q.-S. Jia, and X. Guan, "Optimal control of multiroom hvac system: An event-based approach," *IEEE Transactions on Control Systems Technology*, vol. 24, no. 2, pp. 662–669, 2016.

[4] R. Maddalena, M. Mendell, K. Eliseeva, W. Chan, D. Sullivan, M. Russell, U. Satish, and W. Fisk, "Effects of ventilation rate per person and per floor area on perceived air quality, sick building syndrome symptoms, and decision-making," *Indoor air*, vol. 25, no. 4, pp. 362–370, 2015.

[5] P. O. Fanger *et al.*, "Thermal comfort. analysis and applications in environmental engineering." *Thermal comfort. Analysis and applications in environmental engineering.*, 1970.

[6] J. Lin, W. Yu, N. Zhang, X. Yang, H. Zhang, and W. Zhao, "A survey on internet of things: Architecture, enabling technologies, security and privacy, and applications," *IEEE Internet of Things Journal*, vol. 4, no. 5, pp. 1125–1142, 2017.

[7] L. Liu, Z. Chang, X. Guo, S. Mao, and T. Ristaniemi, "Multiobjective optimization for computation offloading in fog computing," *IEEE Internet of Things Journal*, vol. 5, no. 1, pp. 283–294, 2018.

[8] Y. Wang, S. Mao, and R. M. Nelms, "Distributed online algorithm for optimal real-time energy distribution in the smart grid," *IEEE Internet of Things Journal*, vol. 1, no. 1, pp. 70–80, 2014.

[9] N. Seydoux, K. Drira, N. Hernandez, and T. Monteil, "Autonomy through knowledge: how iot-o supports the management of a connected apartment," in *Semantic Web Technologies for the Internet of Things (SWIT)*. CEUR-WS, 2016.

[10] K. Zhang, J. Ni, K. Yang, X. Liang, J. Ren, and X. S. Shen, "Security and privacy in smart city applications: Challenges and solutions," *IEEE Communications Magazine*, vol. 55, no. 1, pp. 122–129, 2017.

[11] M. Chen, S. Mao, and Y. Liu, "Big data: A survey," *Mobile networks and applications*, vol. 19, no. 2, pp. 171–209, 2014.

[12] G. Hinton, L. Deng, D. Yu *et al.*, "Deep neural networks for acoustic modeling in speech recognition: The shared views of four research groups," *IEEE Signal Processing Magazine*, vol. 29, no. 6, pp. 82–97, 2012.

[13] Y. LeCun, Y. Bengio, and G. Hinton, "Deep learning," *nature*, vol. 521, no. 7553, p. 436, 2015.

[14] A. C. Megri, I. E. Naqa, and F. Haghighat, "A learning machine approach for predicting thermal comfort indices," *International journal of ventilation*, vol. 3, no. 4, pp. 363–376, 2005.

[15] S. Atthajariyakul and T. Leephakpreeda, "Neural computing thermal comfort index for hvac systems," *Energy Conversion and Management*, vol. 46, no. 15-16, pp. 2553–2565, 2005.

[16] ASHRAE Standard, "55 (2010)," *Thermal environmental conditions for human occupancy*, 2010.

[17] T. Chaudhuri, D. Zhai, Y. C. Soh, H. Li, and L. Xie, "Random forest based thermal comfort prediction from gender-specific physiological parameters using wearable sensing technology," *Energy and Buildings*, vol. 166, pp. 391–406, 2018.

[18] E. L. Kruger and P. Drach, "Identifying potential effects from anthropometric variables on outdoor thermal comfort," *Building and Environment*, vol. 117, pp. 230–237, 2017.

[19] W. Hu, Y. Wen, K. Guan, G. Jin, and K. J. Tseng, "itcm: Towards learning-based thermal comfort modeling via pervasive sensing for smart buildings," *IEEE Internet of Things Journal*, 2018.

[20] A. Javed, H. Larijani, A. Ahmadinia, R. Emmanuel, M. Mannion, and D. Gibson, "Design and implementation of a cloud enabled random neural network-based decentralized smart controller with intelligent sensor nodes for hvac," *IEEE Internet of Things Journal*, vol. 4, no. 2, pp. 393–403, 2017.

[21] L. Yu, D. Xie, T. Jiang, Y. Zou, and K. Wang, "Distributed real-time hvac control for cost-efficient commercial buildings under smart grid environment," *IEEE Internet of Things Journal*, vol. 5, no. 1, pp. 44–55, 2018.

[22] J. Langevin, P. L. Gurian, and J. Wen, "Tracking the human-building interaction: a longitudinal field study of occupant behavior in air-conditioned offices," *Journal of Environmental Psychology*, vol. 42, pp. 94–115, 2015.

[23] T.-P. Lin, A. Matzarakis, and R.-L. Hwang, "Shading effect on long-term outdoor thermal comfort," *Building and Environment*, vol. 45, no. 1, pp. 213–221, 2010.

[24] R. P. Kramer, H. L. Schellen, and J. van Schijndel, "Towards temperature limits for museums: a building simulation study for four museum zones with different quality of envelopes," *Proceedings of Healthy Buildings Europe (Eindhoven, 2015)*, 2015.

[25] R. Wooten, "Statistical analysis of the relationship between wind speed, pressure and temperature," *Journal of Applied Sciences*, vol. 11, no. 15, pp. 2712–2722, 2011.